Kristen A. McLaurin, Hailong Li, Charles F. Mactutus and Rosemarie M. Booze*

Constitutive expression of HIV-1 viral proteins induces progressive synaptodendritic alterations in medium spiny neurons: implications for substance use disorders

https://doi.org/10.1515/nipt-2023-0008 Received March 30, 2023; accepted June 26, 2023; published online July 11, 2023

Abstract

Objectives: Perinatally-infected adolescents living with HIV-1 (pALHIV) appear uniquely vulnerable to developing substance use disorders (SUD). Medium spiny neurons (MSNs) in the nucleus accumbens core (NAcc), an integrator of cortical and thalamic input, have been implicated as a key structural locus for the pathogenesis of SUD. To date, however, how constitutive expression of HIV-1 viral proteins alters the development of MSNs in the NAcc has not been systematically evaluated.

Methods: An innovative ballistic labeling technique was utilized to examine MSNs in the NAcc, and associated dendritic spines, in HIV-1 transgenic (Tg) and control animals. First, a time-sequential longitudinal experimental design was implemented, whereby animals were sacrificed at 30-day intervals from postnatal day (PD) 30 to PD 180. Second, the therapeutic efficacy of S-Equol for HIV-1-associated synaptic dysfunction in MSNs was evaluated using a cross-sectional experimental design.

Results: Constitutive expression of HIV-1 viral proteins disrupted the development of MSNs, evidenced by alterations in neuritogenesis and synaptogenesis. Furthermore, age-related, progressive synaptodendritic alterations were observed in the patterning of dendritic branches and dendritic spines, as well as dendritic spine head diameter, in HIV-1 Tg, relative to control, animals. Treatment with S-Equol during the formative period, however, led to long-term enhancements in synaptic function (i.e., PD 180).

Kristen A. McLaurin, Hailong Li and Charles F. Mactutus, Cognitive and Neural Science Program, Department of Psychology, Barnwell College, University of South Carolina, Columbia, SC, USA

Conclusions: Developmental and progressive synaptodendritic alterations in MSNs induced by chronic HIV-1 viral protein exposure may underlie the increased propensity for pALHIV to develop SUD. Elucidating a potential neural mechanism underlying the unique vulnerability of pALHIV to SUD affords a fundamental opportunity for the evaluation of therapeutics.

Keywords: human immunodeficiency virus type 1 (HIV-1); medium spiny neurons; nucleus accumbens; S-Equol; substance use disorders

Introduction

The growing population (approximately 2.7 million [1]) of children and adolescents living with either perinatally or horizontally acquired human immunodeficiency virus type 1 (HIV-1) appear uniquely vulnerable to developing problematic substance use. Indeed, substance use disorders (SUD) are observed in 19–25 % [2, 3] of perinatally-infected adolescents living with HIV-1 (pALHIV); a SUD rate that is three times higher than the adolescent population (i.e., 6.3 %; [4]). Critically, adolescent substance use amongst pALHIV is associated with multiple adverse consequences, including increased disease severity (i.e., lower CD 4 %; [5]), decreased medication adherence [6] and increased sexual risk behaviors [3]. Thus, there is a fundamental need to elucidate the neural mechanism(s) underlying the unique vulnerability of pALHIV to SUD.

The nucleus accumbens (NAc), which is implicated in the pathogenesis of SUD (for review, [7]), is a specialized component of the ventral striatum that serves as a central integrator of cortical and thalamic input (for review, [8]). Anatomically, the NAc is a heterogeneous brain region consisting of at least two subdivisions, including a lateral core region (i.e., the nucleus accumbens core [NAcc]) and a medial shell; a subterritorial organization that was initially demonstrated by region specific efferent projections [9] and histochemistry [10]. The NAcc, in particular, sends

^{*}Corresponding author: Rosemarie M. Booze, PhD, Carolina Trustees Professor and Bicentennial Endowed Chair of Behavioral Neuroscience, Cognitive and Neural Science Program, Department of Psychology, Barnwell College, University of South Carolina, 1512 Pendleton Street, Columbia, SC 29208, USA, E-mail: booze@mailbox.sc.edu

efferent projections to multiple brain regions, including the lateral hypothalamus, lateral ventral pallidum, and substantia nigra [11]. In turn, the NAcc is innervated by afferents from the amygdala, hippocampus, prefrontal cortex (PFC), thalamus, and ventral tegmental area (VTA; [12, 13]). Efferent projections from and afferent projections to the NAc, irrespective of subregion, synapse on inhibitory medium spiny neurons (MSNs); a neuronal type implicated in SUD (for review, [14]). Investigating the development of MSNs in the NAcc, therefore, may elucidate a key structural locus underlying the unique vulnerability of pALHIV to SUD.

MSNs of the NAc are medium-sized neurons that are morphologically characterized by extensive, centrifugal dendritic arborization [15]. Excitatory afferent projections to MSNs uniquely target either proximal or distal dendrites, whereby glutamatergic and dopaminergic synapses are primarily formed on distal dendrites (for review, [16]). Proximal dendrites, in sharp contrast, are innervated with afferents from other MSNs (for review, [17]). In addition, the surface of MSNs is studded with an abundance of dendritic spines [15]; protrusions that serve as the primary postsynaptic compartment for excitatory synapses (for review, [18]). Dendritic spines can be divided into two components, including: (1) a small, spherical head containing the postsynaptic density (PSD); and (2) a thin neck that connects the bulbous head to the dendritic shaft. Morphological parameters of the dendritic spine head and neck fall along a continuum and have been strongly associated with synaptic function [19-22]. Taken together, examination of the structural characteristics, including dendritic branching and dendritic spines, in MSNs of the NAc affords an opportunity to infer neuronal and synaptic function, as well as evaluate novel therapeutics.

Treatment with estrogenic compounds (e.g., 17β-estradiol) induces prominent alterations to neuronal and dendritic spine structure in the NAcc [23-34] supporting an innovative means to remodel neuronal circuitry [24]; the carcinogenic nature of 17β-estradiol [e.g., 25-27], however, limits its translational utility. Plant-derived polycyclic phenols, or phytoestrogens, whose chemical structure resembles 17β-estradiol [28], however, may afford an alternative strategy to target estrogen receptors. Indeed, the phytoestrogen S-Equol (SE), permeates the blood-brain barrier [29], exhibits selective affinity for estrogen receptor β (ER β ; [30, 31]), and serves as a neuroprotective and/or neurorestorative therapeutic for HIV-1-associated neurocognitive [32-34] and affective [35] alterations. Specifically, SE serves as an efficacious treatment for cocaine-seeking behavior, in ovariectomized female HIV-1 transgenic rats [35]; i.e., a biological system

expressing seven of the nine HIV-1 genes constitutively throughout development [36]. The neural mechanism by which SE exerts its therapeutic effects, however, remains understudied.

In light of previous studies, the aims of the present study were two-fold. First, using a time-sequential longitudinal experimental design, to evaluate how constitutive expression of HIV-1 viral proteins (i.e., as in the HIV-1 Tg rat) alters the development of MSNs, and associated dendritic spines, in the NAcc. Cross-sectional studies during adulthood [37, 38] and advanced age [39] have revealed profound structural and functional alteration in MSNs; the experimental design of prior work, however, precludes inferences regarding developmental processes [40]. Second, using a cross-sectional experimental design, to establish the utility of SE to induce long-term enhancements to MSNs of the NAcc and associated dendritic spines in HIV-1 Tg rats. Elucidating a potential neural mechanism underlying the unique vulnerability of pALHIV to SUD affords a fundamental opportunity for the evaluation of therapeutic treatments.

Materials and methods

Animals

Control and HIV-1 Tg animals were bred on a Fischer F344/N background, whereby control animals were procured from Envigo Laboratories (Indianapolis, IN, USA) and HIV-1 Tg animals were bred (control female paired with an HIV-1 Tg male) at the University of South Carolina. Animals of the same sex were pair- or group-housed until sacrifice and had ad libitum access to food (Pro-Lab Rat, Mouse, Hamster Chow #3000) and water.

HIV-1 Tg and control animals were maintained in AAALACaccredited facilities using the guidelines established in the Guide for the Care and Use of Laboratory Animals of the National Institutes of Health. Environmental conditions for the animal colony were targeted at: 21° \pm $2 \,^{\circ}$ C, $50 \,^{\circ}$ $\pm \, 10 \,^{\circ}$ relative humidity and a 12-h light: 12-h dark cycle with lights on at 0700 h (EST). The University of South Carolina Institutional Animal Care and Use Committee (IACUC) approved the project protocol under federal assurance (#D16-00028).

Experiment #1: Time-sequential longitudinal examination of medium spiny neurons in the nucleus accumbens core

A time-sequential longitudinal experimental design was utilized to evaluate how constitutive expression of HIV-1 viral proteins disrupts the development of MSNs in the NAcc. HIV-1 Tg and control animals, with sample sizes of approximately n=40 at each age (Control: Male, n=10, Female, n=8-10; HIV-1 Tg: Male, n=10, Female, n=10) were sacrificed at 30 day intervals from PD 30 to PD 180. MSNs were visualized using a fluorescent neuronal labeling technique and analyzed using sophisticated neuronal reconstruction software (Figure 1).

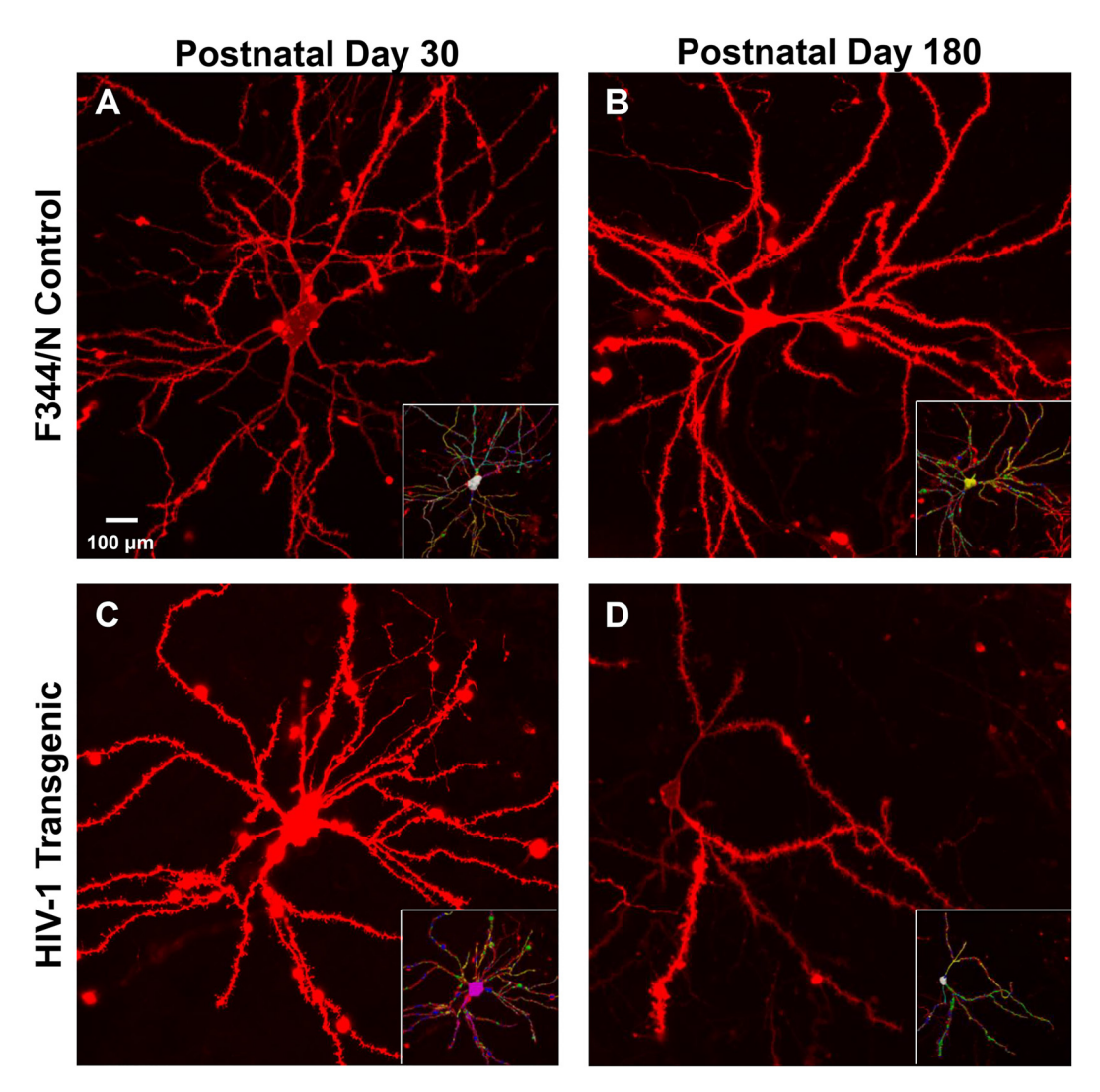


Figure 1: Representative confocal images of ballistically labeled medium spiny neurons in the nucleus accumbens core, and their respective tracings (inset), are shown for F344/N control (A, B) and HIV-1 transgenic (C, D) animals at postnatal day 30 (A, C) and 180 (B, D).

Staging of the estrous cycle: The stage of the estrous cycle was determined in female rats immediately prior to sacrifice using a vaginal lavage. Cytological assessments of vaginal smears were conducted using a 10× light microscope to determine the predominant cell type. A rat whose vaginal smear consisted of predominantly leukocytes was in the diestrus phase of the estrous cycle [41]. To decrease potential variability associated with estrous cycle, we aimed to sacrifice female animals during the diestrus phase.

Fluorescent neuronal labeling technique: A detailed step-by-step protocol for the ballistic labeling technique utilized in our laboratory was published by Li et al. [42].

Preparation of DiOlistic cartridges: In brief, Tefzel tubing (Bio-Rad, Hercules, CA, USA) was filled with a polyvinylpyrrolidone (PVP) solution (i.e., 100 mg PVP dissolved in 10 mL ddH $_2$ O) for 20 min; the solution was then expelled. DiOlistic cartridges were prepared using tungsten beads (170 mg; Bio Rad) and DiIC18(3) dye (6 mg; Invitrogen, Carlsbad, CA, USA), which were individually dissolved in 250 or 300 μL of 99.5 % methylene chloride (Sigmal-Aldrich, St. Louis, MO, USA), respectively.

The tungsten bead suspension and DilC18(3) dye solution were mixed, sonicated, and drawn into the previously prepared PVP-coated Tefzel tubing to create the DiOlistic cartridge. The DiOlistic cartridge was loaded into the tubing preparation station (Bio-Rad) and rotated for 1 min before all water was removed. Rotating, under 0.5 L/min of nitrogen gas, continued for an additional 30 min. The DiOlistic cartridge was cut into 13 mm lengths.

Tissue preparation: Anesthesia was induced in HIV-1 Tg and control animals using 5 % sevoflurane (Abbot Laboratories, North Chicago, IL, USA). Rats were humanely sacrificed using transcardial perfusion and the entire brain was removed and postfixed (4 % paraformaldehyde) for 10 min. A rat brain matrix (ASI Instruments, Warren, MI, USA) was utilized to cut 500 µm coronal slices, which were then placed into a 24 well-plate with 100 mM phosphate-buffered saline (PBS).

Ballistic labeling: The Helios Gene Gun (Bio-Rad) was loaded with previously prepared DiOlistic cartridges and connected to helium gas (Output Pressure: 90 pounds per square inch). The applicator was placed approximately 1.5 cm away from the brain section and fired. After labeling, brain slices were washed three times with 100 mM PBS, stored in the dark at 4 °C for 3 h, and mounted (Pro-Long Gold Antifade, Invitrogen, Waltham, MA, USA) onto a glass slide.

Confocal imaging of medium spiny neurons: Z-stack images of MSNs in the NAcc (3.24-0.48 mm anterior to Bregma; [43]) were obtained for analysis. Specifically, a Nikon TE-2000E confocal microscope, in combination with Nikon's EZ-C1 software (version 3.81b), was utilized to acquire three neuronal images from each animal using the following conditions: $60 \times$ oil objective (n.a.=1.4), Z-plane interval of 0.15 μ m, and a green helium-neon laser (Emission: 543 nm).

Neuronal analysis and spine quantification: Analyses were conducted on neurons blinded to tissue genotype and on one neuron from each animal. Selection of only one neuron per animal, which was conducted using the criteria established by Li et al. [42], precludes the violation of the assumption of independence. Neurons failing to meet the established selection criteria were not included in the analysis, yielding the following sample sizes for analysis at age: Control: PD 30, n=20 (Male, n=10; Female, n=10), PD 60, n=20 (Male, n=10; Female, n=10), PD 90, n=18 (Male, n=10; Female, n=8), PD 120, n=20 (Male, n=10; Female, n=10), PD 150, n=17 (Male, n=8; Female, n=9), PD 180, n=18 (Male, n=10; Female, n=8); HIV-1 Tg: PD 30, n=20 (Male, n=10; Female, n=10), PD 60, n=18 (Male, n=9; Female, n=9), PD 90, n=20 (Male, n=10; Female, n=10), PD 120, n=19, (Male, n=10; Female, n=9), PD 150, n=20 (Male, n=10; Female, n=10), PD 180, n=20 (Male, n=10; Female, n=10).

Following selection, Neurolucida360 (MicroBrightfield, Williston, VT, USA), a sophisticated neuronal reconstruction software, was utilized for the examination of neuronal and dendritic spine morphology. Neuronal morphology was evaluated using two complementary approaches, including total dendrite length and centrifugal branch ordering. In the centrifugal branch ordering method, an evaluation of dendritic branching complexity, a dendrite emanating from the soma is labeled as first-order and each subsequent dendritic bifurcation is increased by one branch order. Analyses were conducted on branch orders one through ten.

Dendritic spine morphological parameters were evaluated along a continuum. Boundary conditions for dendritic spine backbone length (0.2–4.0 μm [44]), volume (0.05–0.85 μm^3 [18]) and head diameter (0.0–1.2 μm; [45]), were selected using well-accepted previously published results. Dendritic spines failing to meet any of the boundary conditions were excluded from dendritic spine morphological analyses.

Experiment #2: therapeutically targeting synaptic dysfunction in medium spiny neurons in the nucleus accumbens core

A cross-sectional experimental design was implemented to evaluate the therapeutic efficacy of SE for enhancing synaptic function in MSNs of the NAcc in HIV-1 Tg animals.

S-Equol treatment: Beginning at approximately PD 28, male (n=9) and female (n=3) HIV-1 Tg animals were treated with a daily oral dose of 0.2 mg of SE (Cayman Chemical Company, Ann Arbor, MI, USA), which was incorporated into sucrose pellets (Bio-Serv, Inc., Flemington, NJ, USA). The SE dose of 0.2 mg was selected for two primary

reasons, including: (1) A dose-response experimental paradigm established 0.2 mg of SE as the most effective dose for mitigating neurocognitive deficits in sustained attention in the HIV-1 Tg rat [32]; and (2) The dose, which yielded a daily amount of 0.25-1.0 mg/kg/SE (i.e., approximately 2.5-10 mg in a 60 kg human), is translationally relevant (i.e., well below the daily isoflavone intake of most elderly Japanese; [46]). Daily oral treatment continued through PD 90.

Staging of the estrous cycle: Estrous cyclicity was evaluated in female animals immediately prior to sacrifice using the methodology detailed in Experiment #1.

Fluorescent neuronal labeling technique: The fluorescent neuronal labeling technique described above was utilized to label MSNs of the NAcc in HIV-1 Tg animals treated with SE. Animals were sacrificed at PD 180. Furthermore, methodology reported above was used for the selection and analysis of MSNs of the NAcc. Neurons failing to meet the established selection criteria were not included in the analysis, yielding the following sample sizes: HIV-1 Tg, n=10 (male, n=9; female, n=1).

Statistical analysis

Analysis of variance (ANOVA) and regression approaches were implemented to statistically analyze data from MSNs in the NAcc. An alpha criterion of p≤0.05 was established for statistical significance.

In Experiment #1: Time-Sequential Longitudinal Examination of Medium Spiny Neurons in the Nucleus Accumbens Core, neurodevelopmental and progressive synaptodendritic alterations were evaluated using both continuous and count dependent variables. Regression approaches (GraphPad Software, Inc., La Jolla, CA, USA) were utilized to examine the development of dendrite length, excitatory synapses, and dendritic patterning. Age-related changes in dendritic patterning were also evaluated using mean branch order, which was statistically analyzed using a univariate ANOVA (SPSS Statistics 27, IBM Corp., Somer, NY, USA). The number of dendritic branches or dendritic spines at branch orders one through ten served as dependent variables for the evaluation of dendritic patterning and the number of excitatory synapses/location of dendritic spines, respectively. Dendritic spine head diameter was analyzed by evaluating the number of dendritic spines within each bin; only dendritic spines with a head diameter greater than $0.01\,\mu m$ were included in the analysis. Dendritic patterning, the location of dendritic spines, and dendritic spine head diameter were analyzed using a generalized linear mixed-effects model with a random intercept, Poisson distribution, and unstructured covariance structure (PROC GLIMMIX; SAS/STAT Software 9.4, SAS Institute, Inc., Cary, NC, USA). For all analyses, genotype (HIV-1 Tg vs. Control), sex (Male vs. Female) and age (Location of Dendritic Spines: PD 30 vs. PD 180; Dendritic Patterning and Dendritic Spine Morphology: PD 30 vs. PD 60 vs. PD 90 vs. PD 120 vs. PD 150 vs. PD 180) served as betweensubjects factors. Branch order or bin served as within-subjects factors, as appropriate.

In Experiment #2: Therapeutically Targeting Synaptic Dysfunction in Medium Spiny Neurons in the Nucleus Accumbens Core, a priori hypotheses were addressed using two planned comparisons to establish: (1) the treatment effect (i.e., HIV-1 Tg vs. HIV-1 Tg SE); and (2) the magnitude of the treatment effect (i.e., Control vs. HIV-1 Tg SE). Analytic approaches for dendritic patterning, the location of dendritic spines, and dendritic spine head diameter are consistent with those implemented for Experiment #1. Treatment (None vs. SE) or genotype (HIV-1 Tg vs. Control) served as the between-subjects factor, whereas branch order or bin served as the within-subjects factor, as appropriate. Biological sex was not included as a between-subjects factor to address the *a priori* hypotheses in Experiment #2 due to low statistical power.

Results

Experiment #1: Time-sequential longitudinal examination of medium spiny neurons in the nucleus accumbens core

HIV-1 Tg animals exhibited profound, early alterations in neurite and dendritic spine development in medium spiny neurons of the nucleus accumbens core

Independent of biological sex, HIV-1 Tg animals exhibited an altered development of total dendrite length, an index of neurite growth, relative to control animals (Figure 2A). Specifically, early in development (i.e., PD 30-PD 90), the total dendrite length in MSNs of HIV-1 Tg rats was greater than control animals. Across development (i.e., PD 90-PD 180), however, total dendrite length regressed in HIV-1 Tg animals (Best Fit: Segmental Linear Regression, $R^2 \ge 0.92$, n=17-20 per genotype at each age). In sharp contrast, dendrite length across development in control animals was well-maintained, whereby total dendrite length was well-described by a horizontal line.

Developmental alterations were further evidenced by an examination of the number of dendritic spines, a proxy for the number of excitatory synapses (for review, [47]). Indeed, presence of the HIV-1 transgene interrupts the development of excitatory synapses, evidenced by agerelated alterations in the total number of dendritic spines (Figure 2B; Generalized Linear Mixed-Effects Model: Genotype \times Age Interaction, F(5, 207)=6.1, p \leq 0.001). Specifically, HIV-1 Tg animals exhibited an initial abundance (i.e., PD 30 and PD 60) and subsequent dramatic decrease in the number of dendritic spines across development; a developmental trajectory that was well-described by a segmental linear regression ($R^2 \ge 0.93$). In control animals, however, the total number of dendritic spines remained stable across development (Best Fit: Horizontal Line). Taken together, constitutive expression of HIV-1 viral proteins profoundly disrupts early developmental processes, including both neuritogenesis and synaptogenesis (i.e., the establishment, maintenance, and/or elimination of neuritic processes and synapses, respectively).

Age-related, progressive alterations in dendritic patterning were observed in HIV-1 Tg, relative to control, animals

A centrifugal branch ordering scheme was utilized to evaluate neuronal morphology, which is functionally associated with the firing properties of neurons [48, 49], of MSNs in the NAcc. Indeed, constitutive expression of HIV-1 viral proteins induced age-related, progressive alterations in dendritic patterning, evidenced by a progressive, linear decrease in mean branch order throughout development (Figure 3A; Univariate ANOVA: Genotype × Age Interaction,

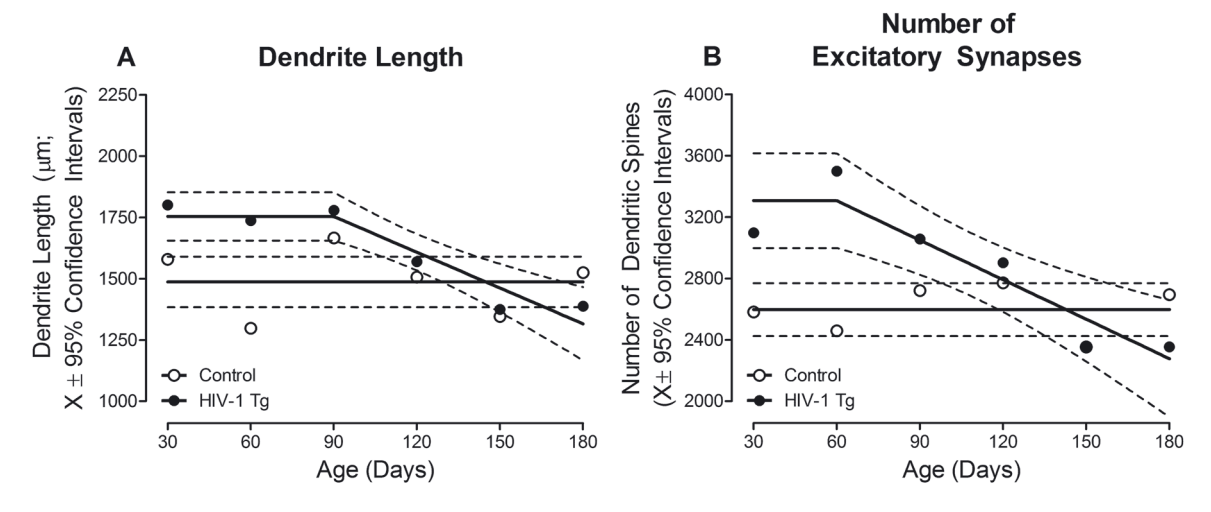


Figure 2: Neurodevelopmental alterations in neuritogenesis and synaptogenesis were observed in HIV-1 Tg rats. Specifically, HIV-1 Tg animals exhibited an initial increase in dendrite length (A) and the number of dendritic spines (B) early in development; parameters which subsequently decreased across time (X \pm 95 % confidence intervals). In sharp contrast, dendrite length and the number of dendritic spines were stable across development in control animals.

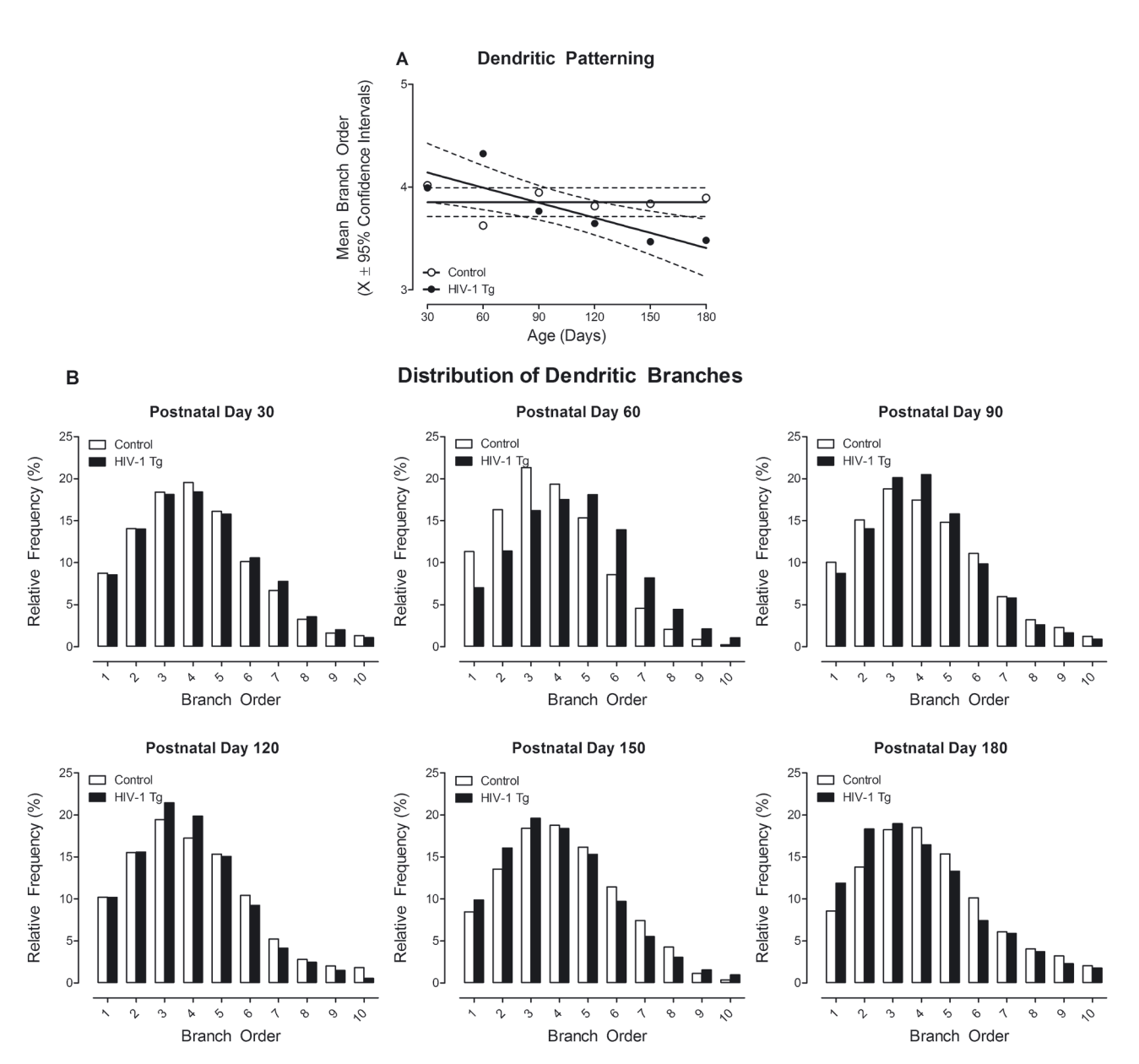


Figure 3: An abnormal patterning of dendritic branches in medium spiny neurons of the nucleus accumbens core was observed in HIV-1 Tg animals. (A) Mean branch order (X ± 95 % confidence intervals) was derived from the distribution of dendritic branches. A linear decrease in mean branch order was observed in HIV-1 Tg animals across development; a sharp contrast to the well-maintained patterning of dendritic branches observed in control animals. (B) Inferences drawn from the examination of mean branch order were confirmed in HIV-1 Tg and control animals by evaluating the distribution of dendritic branches as a function of age. Data are illustrated as relative frequencies of the entire dendritic spine population.

F(5, 206)=2.3, p≤0.05, η_p^2 =0.053; Best Fit: First-Order Polynomial, R²s≥0.71); dendritic patterning in control animals, however, was well-maintained across development (Best Fit: Horizontal Line). Examination of the distribution of dendritic branches (Figure 3B) confirmed the age-related alteration in dendritic patterning (Generalized Linear Mixed-Effects Model: Genotype × Age × Branch Order Interaction, F(45, 1857)=2.4, p≤0.001). Specifically, HIV-1 Tg, relative to

control, animals exhibited an increased relative frequency of higher-order dendritic branches at PD 30 and PD 60. A population shift, with an increased relative frequency of lower-order dendritic branches, however, was observed in HIV-1 Tg animals at PD 120, PD 150, and PD 180. Morphological alterations in the MSNs of HIV-1 Tg animals, therefore, may reflect changes in the firing properties of these neurons.

HIV-1 Tg animals exhibited an age-related population shift in the location of dendritic spines on medium spiny neurons

A prominent age-related population shift in the distribution of dendritic spines on dendritic branches was observed in HIV-1 Tg, relative to control, animals (Figure 4; Generalized Linear Mixed-Effects Model: Genotype × Age × Branch Order Interaction, F(9, 628)=190.9, p<0.001). At PD 30, HIV-1 Tg animals exhibited an increased relative frequency of dendritic spines on higher-order dendritic branches, which receive glutamatergic and dopaminergic projections from the PFC and VTA [16], respectively, relative to control animals. However, a population shift, with an increased relative frequency of dendritic spines on lower-order dendritic branches, which are primarily innervated by afferents from other MSNs [17], was observed in HIV-1 Tg animals at PD 180. The factor of biological sex influenced the magnitude, but not pattern, of the age-related population shift in the location of dendritic spines on MSNs (Generalized Linear Mixed-Effects Model: Genotype \times Sex \times Age \times Branch Order Interaction, F(9, 628)=147.5, p ≤ 0.001). Results support, therefore, age-related changes in neurotransmission in the HIV-1 Tg rat.

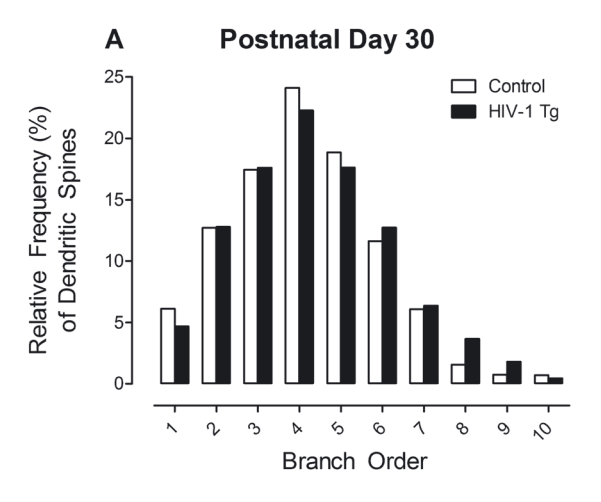
HIV-1 Tg animals displayed an age-related decrease in dendritic spine head diameter from postnatal day 30 to postnatal day 180

Age-related alterations in dendritic spine head diameter, a dendritic spine morphological parameter that is positively correlated with the area of the postsynaptic density [19–21], were observed in HIV-1 Tg, relative to control, animals (Figure 5; Generalized Linear Mixed-Effects Model: Genotype \times Age \times Bin Interaction, F(55, 2,255)=34.3, p \leq 0.001). Specifically, early in development (i.e., PD 30, 60, and 90), HIV-1 Tg animals exhibited a prominent rightward population shift, with an increased relative frequency of dendritic spines with increased head diameter, relative to control animals. At PD 120, 150, and 180, however, HIV-1 Tg, relative to control, animals displayed a profound leftward shift in the distribution of dendritic spine head diameter; a population shift associated with an increased relative frequency of dendritic spines with decreased head diameter. Dendritic spine dysmorphology in HIV-1 Tg animals adds additional evidence for progressive synaptic dysfunction and neurotransmission alterations.

Experiment #2: Therapeutically targeting synaptic dysfunction in medium spiny neurons in the nucleus accumbens core

At postnatal day 180, S-Equol mitigated alterations in the distribution of dendritic branches, dendritic spines, and dendritic spine head diameter in HIV-1 Tg animals

Treatment with SE during the formative period led to long-term enhancements in MSNs of the NAcc, relative to untreated HIV-1 Tg animals, evidenced by a profound population shift in the distribution of dendritic branches, location of dendritic spines, and dendritic spine head diameter (Figure 6A-C). Specifically, HIV-1 Tg ani-



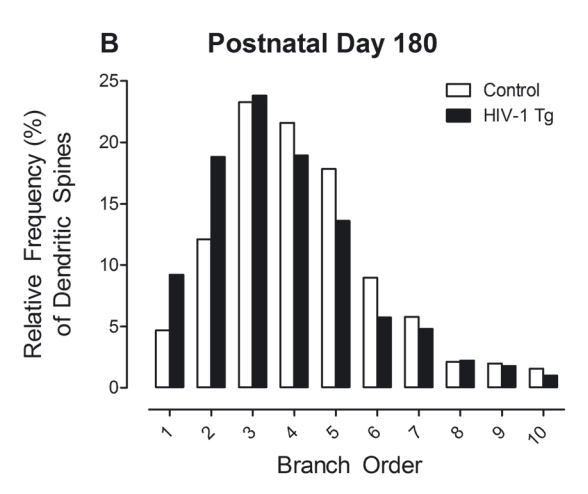


Figure 4: A prominent age-related population shift in the distribution of dendritic spines on dendritic branches was observed in HIV-1 Tg, relative to control, animals. (A) At postnatal day (PD) 30, HIV-1 Tg animals exhibited an increased relative frequencey of dendritic spines on higher order branches relative to control animals. (B) A leftward population shift with an increased relative frequency of dendritic spines on lower order branches was observed in HIV-1Tq, relative to control, animals at PD 180. Data are illustrated as relative frequencies of the entire dendritic spine population.

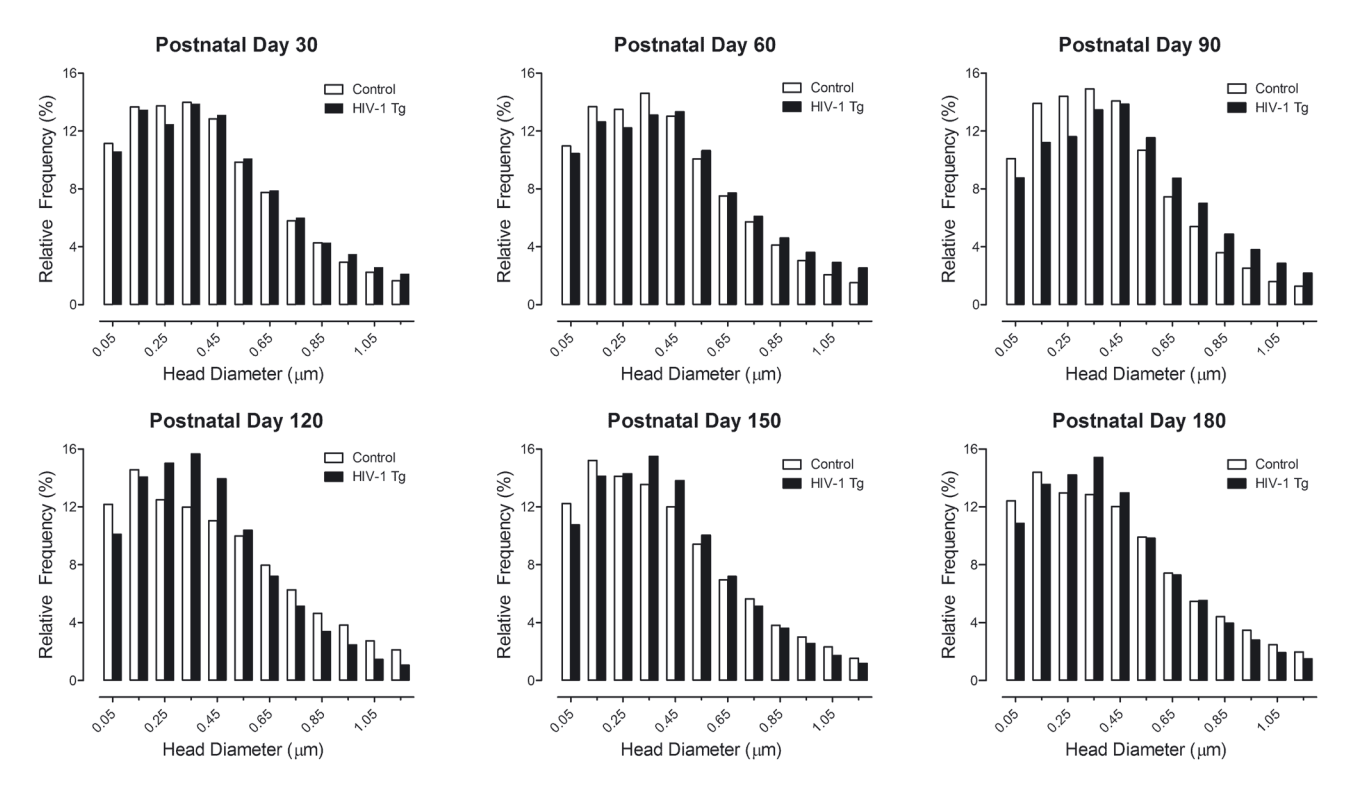


Figure 5: Dendritic spine head diameter was evaluated in HIV-1 Tg and control animals from postnatal day (PD) 30 to PD 180. HIV-1 Tg animals displayed a progressive, age-related decrease in dendritic spine head diameter relative to control animals. Specifically, a population shift towards an increased dendritic spine head diameter was observed in HIV-1 Tg, relative to control, animals at PD 30, 60 and 90. In sharp contrast, HIV-1 Tg animals exhibited a population shift towards a decreased dendritic spine head diameter at PD 120, 150, and 180 relative to control animals. Data are illustrated as relative frequencies of the entire dendritic spine population.

mals treated with SE exhibited an increased relative frequency of higher-order dendritic branches (Generalized Linear Mixed-Effects Model: Treatment \times Branch Order Interaction, F(9, 251)=22.0, $p \le 0.001$) and an increase in the frequency of dendritic spines on higher-order dendritic branches (Generalized Linear Mixed-Effects Model: Treatment \times Branch Order Interaction, F(9, 251)=225.7, $p \le 0.001$), relative to untreated HIV-1 Tg rats. A population shift with an increased relative frequency of dendritic spines with increased head diameter was also observed in HIV-1 Tg SE, relative to untreated, animals (Generalized Linear Mixed-Effects Model: Treatment \times Bin Interaction, F(11, 308)=80.3, $p \le 0.001$).

Furthermore, HIV-1 Tg animals treated with SE were statistically compared to control animals to assess the magnitude of the SE treatment effect (Figure 6D–F). A robust rightward population shift in the distribution of dendritic branches (Generalized Linear Mixed-Effects Model: Genotype \times Branch Order Interaction, F(9, 234)=19.4, p \leq 0.001), location of dendritic spines (Generalized Linear Mixed-Effects Model: Genotype \times Branch Order Interaction, F(9, 234)=45.8, p \leq 0.001), and dendritic spine head diameter (Generalized Linear Mixed-Effects Model: Genotype \times Bin

Interaction, F(11, 275)=82.1, p≤0.001) was observed in HIV-1 Tg SE, relative to control, animals. Collectively, SE treatment during the formative period induced long-term modifications in MSNs of the NAcc consistent with enhancements in synaptic function.

Discussion

Neurodevelopmental and progressive synaptodendritic alterations in MSNs of the NAcc were induced by chronic HIV-1 viral protein exposure (Figure 7). Indeed, alterations in the development of MSNs, and associated dendritic spines, were evidenced in HIV-1 Tg animals by excessive dendrite length and an increased number of dendritic spines, relative to control animals, early in development; parameters which subsequently regressed across time. Age-related, progressive synaptodendritic alterations were observed in the patterning of both dendritic branches and dendritic spines, as well as dendritic spine morphology, in HIV-1 Tg, relative to control, animals. Fundamentally, the profound age-related synaptodendritic alterations observed in HIV-1 Tg rats afforded a target for the evaluation of a novel therapeutic. At PD 180, the phytoestrogen SE mitigated

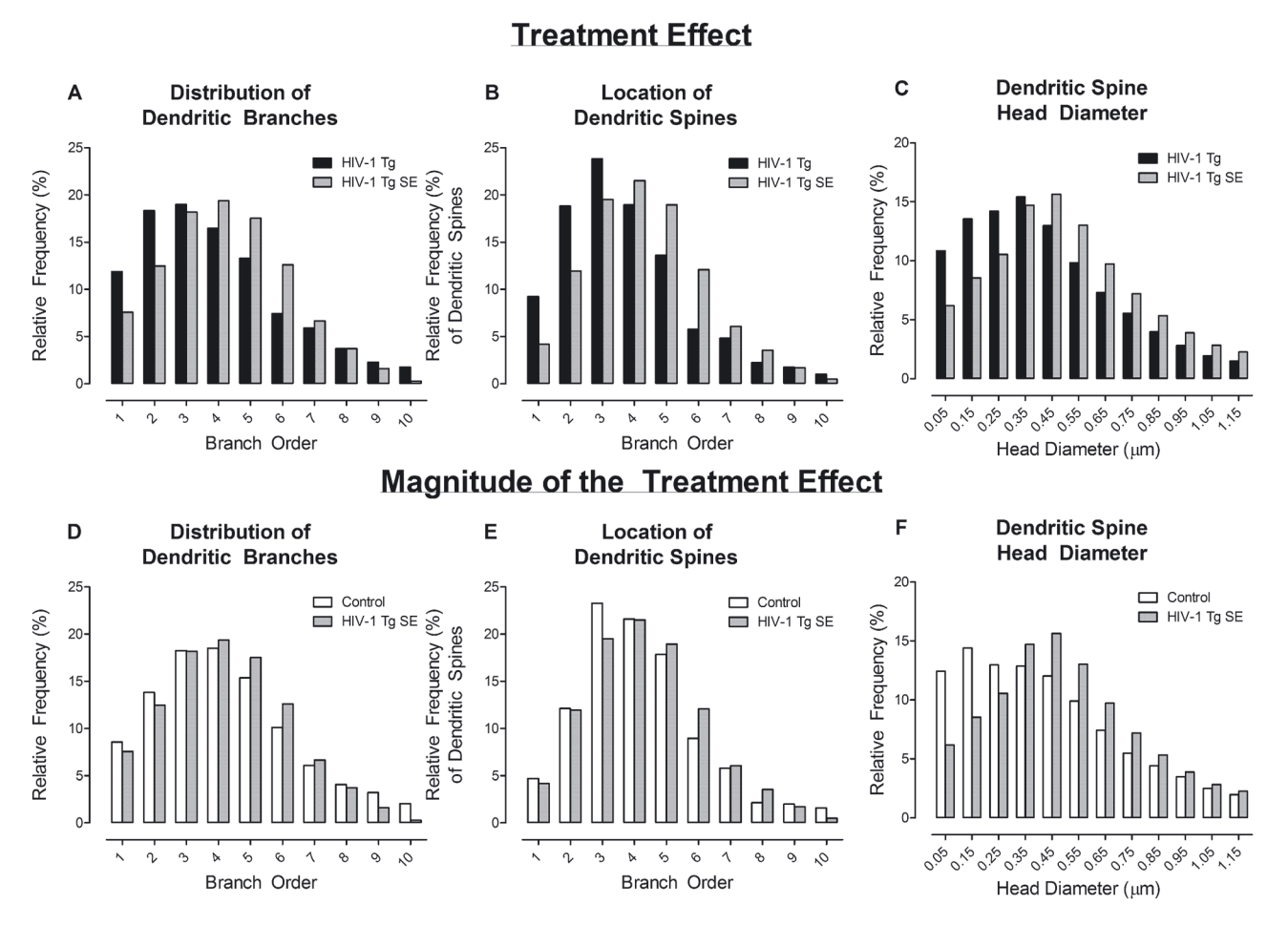


Figure 6: Treatment with S-Equol (SE) during the formative period (i.e., postnatal day [PD] 28-90) mitigates the profound synaptodendritic alterations observed in HIV-1 Tg animals at PD 180. (A-C) A treatment effect was established by comparing HIV-1 Tg animals treated with SE and untreated HIV-1 Tg animals. HIV-1 Tg animals treated with SE exhibited enhanced synaptic function relative to untreated HIV-1 Tg animals, evidenced by a profound rightward population shift in the distribution of dendritic branches, location of dendritic spines, and dendritic spine head diameter. (D-F) The magnitude of the treatment effect was evaluated by comparing HIV-1 Tq animals treated with SE and control animals. A prominent rightward population shift in the distribution of dendritic branches, location of dendritic spines, and dendritic spine head diameter was observed in HIV-1 Tq animals treated with SE relative to control animals. Data are illustrated as relative frequencies of the entire dendritic spine population.

the profound synaptodendritic deficits observed in HIV-1 Tg animals. Collectively, age-related alterations in MSNs induced by constitutive expression of HIV-1 viral proteins may serve as a key structural locus underlying the increased propensity for pALHIV to develop SUD; a structural locus that may be therapeutically targeted by the phytoestrogen SE.

Striatal cells are generated from neuronal progenitors located in the proliferative zones of the ventricular (or ganglionic) eminences [e.g., 50-52]; the lateral ganglionic eminence (LGE), in particular, gives rise to MSNs [53, 54]. Following mitosis, neurons generated in the LGE migrate across short distances to the striatum [55] and undergo prolonged postnatal maturation (i.e., through approximately PD 21 in rodents). Maturation of MSNs is completed by approximately PD 30 in rodents, whereby the dendritic arbor and dendritic spines have stabilized and are indistinguishable from adults [56, 57; Present Study]. Constitutive expression of HIV-1 viral proteins, however, alters the maturation of MSNs, evidenced by delayed neuritogenesis and synaptogenesis.

In addition to early neurodevelopmental alterations, constitutive expression of HIV-1 viral proteins induced an age-related, progressive population shift in dendritic branches and dendritic spines. Across time, HIV-1 Tg animals developed an increased relative frequency of both dendritic branches and dendritic spines on lower order branches relative to control animals; findings which have functional implications for neuronal firing and neurotransmitter innervation. Indeed, computational modeling [48, 49]

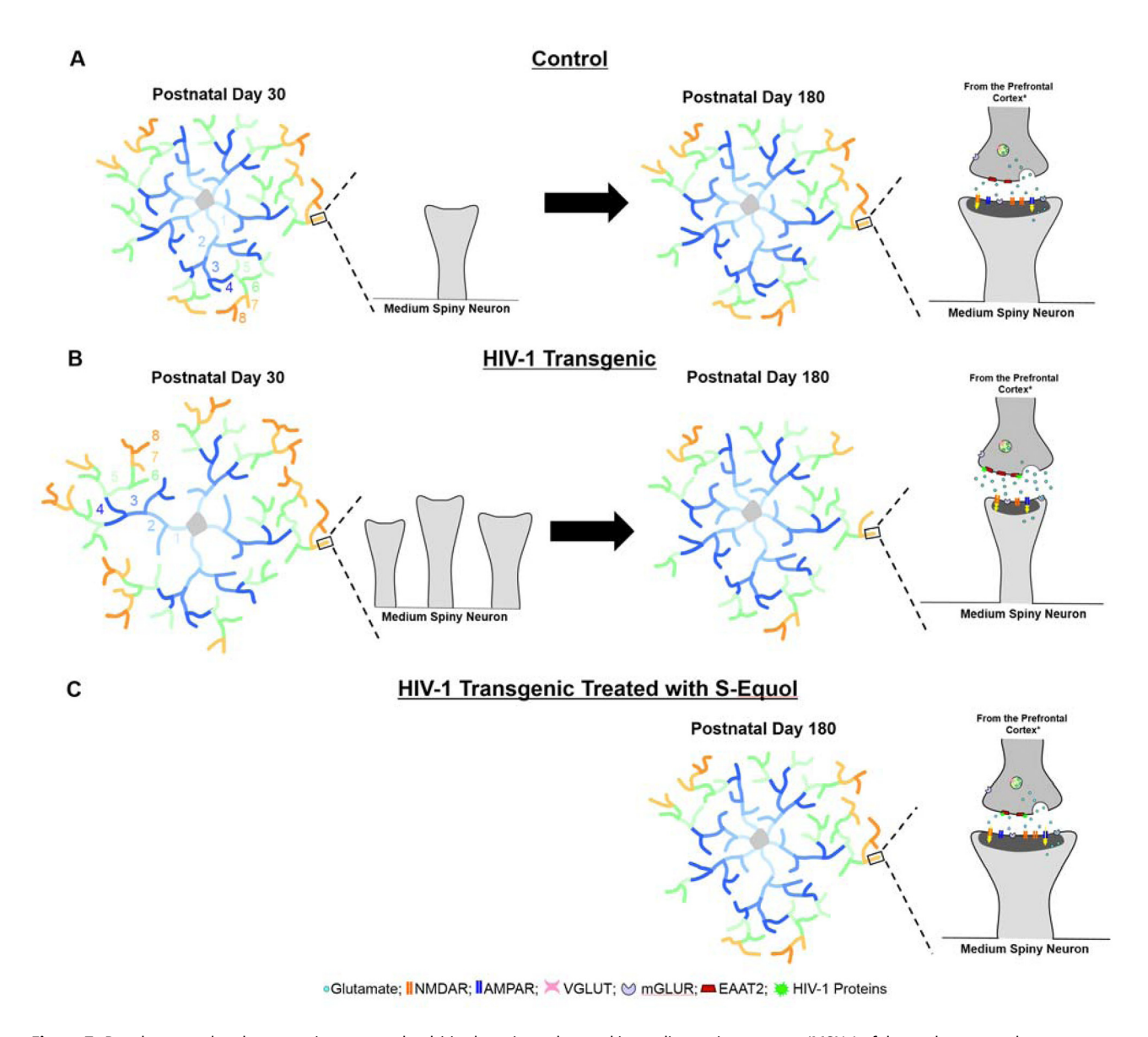


Figure 7: Developmental and progressive synaptodendritic alterations observed in medium spiny neurons (MSNs) of the nucleus accumbens core (NAcc) are illustrated at postnatal day (PD) 30 and PD 180 as a function of genotype (i.e., control vs. HIV-1 Tg) and treatment (i.e., untreated vs. SE). (A) In control animals, morphological parameters (i.e., number of excitatory synapses, dendritic branching) of MSNs are well-established by PD 30 and maintained through adulthood (i.e., PD 180). An increased relative frequency of dendritic spines with greater head diameter, supporting a larger postsynaptic density, are observed in control animals at PD 180 relative to HIV-1 Tg animals. (B) HIV-1 Tg animals, in sharp contrast, exhibited exhuberant dendritic length and number of dendritic spines at PD 30; parameters which subsequently regressed across time. Furthermore, constitutive expression of HIV-1 viral proteins induced an age-related decrease in dendritic spine head diameter from PD 30 to PD 180. (C) Treatment with S-Equol (SE) during the formative period (i.e., PD 28 to PD 90) mitigated the profound synaptodendritic alterations observed in the HIV-1 Tg rat at PD 180. Specifically, HIV-1 Tg animals treated with SE exhibited a pronounced rightward shift in dendritic spine head diameter relative to untreated HIV-1 Tg rats, supporting enhanced synaptic strength.

and *in vivo* preclinical evaluations [49] strongly support the association between dendritic arborization and neuronal firing properties (e.g., afterhyperpolarization, cellular capacitance). Furthermore, the location of dendritic spines has implications for neurotransmission, whereby proximal and distal dendrites in MSNs are innervated by unique afferent projections (i.e., Proximal: Other MSNs; Distal: Glutamatergic and Dopaminergic Afferents from the PFC and VTA, respectively; [16, 17]). Critically, chronic HIV-1 viral protein exposure dysregulates the electrophysiological properties of MSNs [38, 58] and neurotransmission in the NAc [59–62].

Examination of dendritic spine head diameter also revealed additional age-related, progressive synaptic dysfunction in the HIV-1 Tg rat; dysfunction that was supported by a profound decrease in dendritic spine head diameter across development. The postsynaptic density (PSD), which is localized within the dendritic spine head, is a complex biochemical apparatus representing the postsynaptic component of a synapse. From a molecular perspective, the PSD is composed of ionotropic glutamate receptors (e.g., N-methyl-D-aspartate receptors [NMDAR] and α-amino-3-hydroxy-5-methyl-4-isoxazole propionic acid receptors [AMPAR]), cell adhesion and signaling molecules (e.g., N-cadherin and calcium-dependent protein kinase II [CAMKII], respectively), as well as scaffolding proteins (e.g., post-synaptic density 95 [PSD-95]). Characteristics of the PSD can be inferred by examining dendritic spine morphological parameters, as a strong positive association between dendritic spine head volume and area of the PSD has been observed ([19] r=0.55 [20]; r=0.88 [21]; r=0.88 [63]; $r\geq0.76$). Dendritic spine head volume is also significantly correlated with the expression of AMPA-sensitive glutamate receptors [64] and the amplitude of NMDAR-mediated currents [65]. Hence, the progressive decreases in dendritic spine head diameter observed in the HIV-1 Tg rat support age-related reductions in area of the PSD and glutamatergic neurotransmission. The inferences drawn from the morphological parameters of dendritic spines are further supported by previously reported HIV-1 induced alterations in PSD-95 [66, 67] and NMDAR function [e.g. 68, 69].

Neurodevelopmental and progressive synaptodendritic alterations in the HIV-1 Tg rat may result, at least in part, from dysfunction in the Wnt signaling pathway. Generally characterized as morphogens, Wnt proteins are evolutionarily conserved glycoproteins that are encoded by 19 genes in most mammals (for review, [70]). Wnt signaling begins with the binding of Wnt proteins to various membrane receptors (e.g., Frizzled, Ryk), which results in the activation of downstream pathways that are broadly, but not rigorously, classified as either β -catenin-dependent (i.e., canonical) or β -catenin-independent (i.e., non-canonical). One of the key features of the canonical Wnt pathway, specifically, is the enzyme glycogen synthase kinase 3α and 3β (GSK- 3α and GSK- 3β , respectively), which is inhibited by Wnts to activate downstream β-catenin signaling (for review, [71]). Early central nervous system development is dependent upon the integrity of Wnt signaling pathways, evidenced by their role in both dendrite outgrowth [e.g., 72-75] and dendritic spine formation [e.g., 76, 77]. Indeed, alterations to Wnt membrane receptors (i.e., frizzled9 gene: [74]; Ryk receptor: [75]) induce changes

in neuronal structure (i.e., dendrite length, number of dendritic spines) that resemble early neurodevelopmental alterations in the HIV-1 Tg rat. In the mature (i.e., adult) central nervous system, non-canonical Wnt signaling pathways modulate excitatory synapses (for review, [78]). Wnt5a, for example, regulates the structure and function of excitatory postsynaptic sites, evidenced by its role in the clustering of postsynaptic density 95 in dendritic spines [68] and glutamatergic synaptic transmission [79, 80]. Fundamentally, abnormal gene expression in multiple Wnt family members (e.g., Wnt5a, Wnt11) and frizzled class receptors (e.g., FZD4) have been reported in the HIV-1 Tg rat [81] and following HIV-1 infection [e.g., 82]. Exposure to HIV-1 viral proteins also results in the abnormal activation of GSK-3\beta [e.g., 83, 84]. The prominent neurodevelopmental and age-related synaptic dysfunction induced by constitutive expression of HIV-1 viral proteins affords a key target for the development of novel therapeutics.

Long-term modifications in neuronal and dendritic spine structure in MSNs of the NAcc were observed in HIV-1 Tg animals treated with SE during the formative period (i.e., PD 28 to PD 90). Indeed, at PD 180, HIV-1 Tg animals treated with SE exhibited a profound population shift in the distribution of dendritic branches, location of dendritic spines, and dendritic spine head diameter relative to their untreated counterparts; observations which are consistent with enhancements in neuronal firing, neurotransmitter system innervation, and the PSD, respectively. Findings of the present study resemble those following comorbid HIV-1 and SUD (i.e., cocaine self-administration), whereby treatment with SE exerted its therapeutic effects by mitigating synaptodendritic alterations in MSNs of the NAcc [35]. Fundamentally, the enhancement of synaptic function was sufficient to alter drug-seeking behavior, as HIV-1 Tg animals treated with SE exhibited decreased response vigor and drug escalation relative to HIV-1 Tg animals treated with vehicle [35]. SE, via its actions on neuronal and dendritic spine structure, has the potential to reduce the vulnerability of pALHIV to SUD.

Modulation of the Wnt signaling pathway may serve as the mechanism by which SE mitigates synaptodendritic alterations in the HIV-1 Tg rat. Indeed, treatment with the ovarian steroid hormone estradiol inhibits GSK-3\beta in cortical and hippocampal neurons evidenced by a transient increase in phosphorylation at serine 9 [85, 86] and GSK-3 activity [85, 87]. The modification in GSK-3β activity induced by estradiol treatment has downstream effects, whereby an increased accumulation of β-catenin in neuronal cells has been reported [86, 87]. Fundamentally, in neuronal cells both estrogen receptor α and ER β are associated with GSK-3β and β-catenin in a multimolecular complex, whereby estradiol regulates β-catenin via its actions on GSK-3β [85, 86]. Activation of the Wnt/β-catenin pathway, evidenced by increased phosphorylation at serine 9, β-catenin protein expression, or selective increases in Wnt5a expression has also been observed in peripheral cells following treatment with the phytoestrogens (e.g., ASPP 049 [88]; Genistein: [89]). Collectively, treatment with SE, a selective ER β agonist, may mitigate the profound decrease in GSK-3 β phosphorylation at serine 9 induced by exposure to HIV-1 viral proteins [84] resulting in the normalization of β-catenin and central nervous system development.

An innovative ballistic labeling technique, in combination with sophisticated neuronal reconstruction software (i.e., Neurolucida360), was utilized to rigorously examine the population of dendritic spines; a methodology that deserves further consideration. Originally described by Gan et al. [90], ballistic labeling uses specialized equipment (e.g., Helios Gene Gun) to fire microprojectiles (e.g., Tungsten Beads) coated with carbocyanine dyes (e.g., DiO, DiI) into neuronal tissue. Carbocyanide dyes are characterized by two positively-charged conjugated rings and an attached long hydrocarbon chain joined together by a bridge of methine groups. The long hydrocarbon chain, in particular, renders carbocyanide dyes lipophilic; a property that allows for their incorporation into the plasma membrane of neurons [91]. The introduction of carbocyanine dyes via ballistic delivery systems provides clear advantages over more traditional methods (e.g., Golgi-Cox Silver Impregnation, Microinjection), as the approach rapidly and completely labels neuronal cells and associated dendritic spines with minimal tissue damage and no disruption of cellular processes (for review, [92]). High-resolution threedimensional imaging (i.e., using confocal microscopy) is completed to visualize fluorescently labeled neurons; neurons whose structural features (e.g., neuronal branching patterns, dendritic spine morphology) can be precisely measured using sophisticated neuronal reconstruction software [93]. Indeed, it is the accurate, continuous measurements, rather than the classic categorization of dendritic spines, that afforded an opportunity to establish HIV-1-induced population shifts in the morphology of MSNs and their associated dendritic spines.

In conclusion, neurodevelopmental and progressive synaptodendritic alterations were observed in MSNs in the NAcc following constitutive expression of HIV-1 viral proteins. Targeting these alterations with the selective ERB agonist SE during the formative period induces long-term modifications to synaptodendritic structure, whereby MSNs in the NAcc in HIV-1 Tg animals treated with SE resemble control animals at PD 180. Collectively, HIV-1-associated agerelated structural alterations in MSNs may serve as a key structural locus underlying the increased propensity for pALHIV to develop SUD; a structural locus that may be therapeutically targeted by the phytoestrogen SE.

Research funding: This work was supported in part by grants from NIH (National Institute on Drug Abuse, DA013137, DA056288, DA059310; National Institute of Child Health and Human Development, HD043680; National Institute of Mental Health, MH106392; National Institute of Neurological Disorders and Stroke, NS100624) and the interdisciplinary research training program supported by the University of South Carolina Behavioral-Biomedical Interface Program.

Author contributions: All authors have accepted responsibility for the entire content of this manuscript and approved its submission.

Competing interests: Authors state no conflict of interest. Ethical approval: HIV-1 Tg and control animals were maintained in AAALAC-accredited facilities using the guidelines established in the Guide for the Care and Use of Laboratory Animals of the National Institutes of Health. Environmental conditions for the animal colony were targeted at: 21° ± $2 \,^{\circ}$ C, $50 \,^{\circ}$ $\pm \, 10 \,^{\circ}$ relative humidity and a 12-h light: 12-h dark cycle with lights on at 0700 h (EST). The University of South Carolina Institutional Animal Care and Use Committee (IACUC) approved the project protocol under federal assurance (#D16-00028).

References

- 1. HIV and AIDS in adolescents. UNICEF; 2023 [Online]. Available from: https://data.unicef.org/topic/hiv-aids/.
- 2. Abrams EJ, Mellins CA, Bucek A, Dolezal C, Raymond J, Wiznia A, et al. Behavioral health and adult milestones in young adults with perinatal HIV infection or exposure. Pediatrics 2018;142:e20180938.
- 3. Benson S, Elkington KS, Leu CS, Bucek A, Dolezal C, Warne P, et al. Association between psychiatric disorders, substance use, and sexual risk behaviors in perinatally HIV-exposed youth. | Assoc Nurses AIDS Care 2018;29:538-49.
- 4. 2021 national survey of drug use and health (NSDUH) releases. SAMHSA; 2023 [Online]. Available from: https://www.samhsa.gov/data/release/2021-national-surveydrug-use-and-health-nsduh-releases#detailed-tables.
- 5. Williams PL, Leister E, Chernoff M, Nachman S, Morse E, Di Poalo V, et al. Substance use and its association with psychiatric symptoms in perinatally HIV-infected and HIV-affected adolescents. AIDS Behav 2010;14:1072-82.
- 6. Chandwani S, Koenig LJ, Sill AM, Abramowitz S, Conner LC, D'Angelo L. Predictors of antiretroviral medication adherence

- among a diverse cohort of adolescents with HIV. J Adolesc Health 2012;51:242-51.
- 7. Koob GF, Volkow ND. Neurocircuitry of addiction. Neuropsychopharmacology 2010;35:217 – 38.
- 8. Mogenson GJ, Jones DL, Yim CY. From motivation to action: functional interface between the limbic system and the motor system. Prog Neurobiol 1980;14:69-97.
- 9. Groenewegen HJ, Russchen FT. Organization of the efferent projections of the nucleus accumbens to pallidal, hypothalamic, and mesencephalic structures: a tracing and immunohistochemical study in the cat. J Comp Neurol 1984;223:347-67.
- 10. Záborszky L, Alheid GF, Beinfeld MC, Eiden LE, Heimer L, Palkovits M. Cholecystokinin innervation of the ventral striatum: a morphological and radio immunological study. Neuroscience 1985:14:427-53.
- 11. Heimer L, Zahm DS, Churchill L, Kalivas PW, Wohltmann C. Specificity in the projection patterns of accumbal core and shell in the rat. Neuroscience 1991;41:89-125.
- 12. Fallon JH, Moore RY. Catecholamine innervation of the basal forebrain. IV. Topography of the dopamine projection to the basal forebrain and neostriatum. J Comp Neurol 1978;180:545 – 80.
- 13. Ma L, Chen W, Yu D, Han Y. Brain-wide mapping of afferent inputs to accumbens nucleus core subdomains and accumbens nucleus subnuclei. Front Syst Neurosci 2020;14:15.
- 14. Lobo MK, Nestler EJ. The striatal balancing act in drug addiction: distinct roles of direct and indirect pathway medium spiny neurons. Front Neuroanat 2011;5:41.
- 15. Wilson CJ, Groves PM. Fine structure and synaptic connections of the common spiny neuron of the rat neostriatum: a study employing intracellular inject of horseradish perodixase. J Comp Neurol 1980;194:599-615.
- 16. Spiga S, Mulas G, Piras F, Diana M. The "addicted" spine. Front Neuroanat 2014:8:110.
- 17. Groves PM. A theory of the functional organization of the neostriatum and the neostriatal control of voluntary movement. Brain Res 1983;286:109-32.
- 18. Harris KM, Kater SB. Dendritic spines: cellular specializations imparting both stability and flexibility to synaptic function. Annu Rev Neurosci 1994:17:341-71.
- 19. Harris KM, Stevens JK. Dendritic spines of rat cerebellar Purkinje cells: serial electron microscopy with reference to their biophysical characteristics. J Neurosci 1988;8:4455 – 69.
- 20. Harris KM, Stevens JK. Dendritic spines of CA1 pyramidal cells in the rat hippocampus serial electron microscopy with reference to their biophysical characteristics. J Neurosci 1989;9:2982 – 97.
- 21. Arellano JI, Benavides-Piccione R, Defelipe J, Yuste R. Ultrastructure of dendritic spines: correlation between synaptic and spine morphologies. Front Neurosci 2007;1:131-43.
- 22. Araya R, Vogels TP, Yuste R. Activity-dependent dendritic spine neck changes are correlated with synaptic strength. Proc Natl Acad Sci USA 2014;111:E2895 - 904.
- 23. Staffend NA, Loftus CM, Meisel RL. Estradiol reduces dendritic spine density in the ventral striatum of female Syrian hamsters. Brain Struct Funct 2011;215:187 – 94.
- 24. Peterson BM, Mermelstein PG, Meisel RL. Estradiol mediates dendritic spine plasticity in the nucleus accumbens core through activation of mGluR5. Brain Struct Funct 2015;220:2415-22.

- 25. Huseby RA. Demonstration of a direct carcinogenic effect of estradiol on leydig cells of the mouse. Cancer Res 1980;40:1006-13.
- 26. Highman B, Greenman DL, Norvell MJ, Farmer J, Shellenberger TE. Neoplastic and preneoplastic lesions induced in female C3H mice by diets containing diethylstilbestrol or 17 beta-estradiol. J Environ Pathol Toxicol 1980;4:81-95.
- 27. Colditz GA, Hankinson SE, Hunter DJ, Willett WC, Manson JE, Stampfer MJ, et al. The use of estrogens and progestins and the risk of breast cancer in postmenopausal women. N Engl J Med 1995;332:1589-93.
- 28. Glazier MG, Bowman MA. A review of the evidence for the use of phytoestrogens as a replacement for traditional estrogen replacement therapy. Arch Intern Med 2001;161:1161-72.
- 29. Johnson SL, Kirk RD, DaSilva NA, Ma H, Seeram NP, Bertin MJ. Polyphenol microbial metabolites exhibit gut and blood-brain barrier permeability and protect murine microglia against LPS-induced inflammation. Metabolites 2019;9:78.
- 30. Setchell KDR, Clerici C, Lephart ED, Cole SJ, Heenan C, Castellani D, et al. S-Equol, a potent ligand for estrogen receptor beta, is the exclusive enantiomeric form of the soy isoflavone metabolite produced by human intestinal bacterial flora. Am J Clin Nutr 2005;81:1072-9.
- 31. Bertrand SJ, Hu C, Aksenova MV, Mactutus CF, Booze RM. HIV-1 Tat and cocaine mediated synaptopathy in cortical and midbrain neurons is prevented by the isoflavone equal. Front Microbiol 2015;6:894.
- 32. Moran LM, McLaurin KA, Booze RM, Mactutus CF. Neurorestoration of sustained attention in a model of HIV-1 associated neurocognitive disorders. Front Behav Neurosci 2019;13:169.
- 33. McLaurin KA, Moran LM, Booze RM, Mactutus CF. Selective estrogen receptor β agonists: a therapeutic approach for HIV-1 associated neurocognitive disorders. | Neuroimmune Pharmacol 2020:16:264-79
- 34. McLaurin KA, Li H, Cook AK, Booze RM, Mactutus CF. S-Equol: a neuroprotective therapeutic for chronic neurocognitive impairments in pediatric HIV. J Neurovirol 2020;26:704-18.
- 35. McLaurin KA, Bertrand SJ, Illenberger JM, Harrod SB, Mactutus CF, Booze RM. S-Equol mitigates motivational deficits and dysregulation associated with HIV-1. Sci Rep 2021;11:11870.
- 36. Reid W, Sadowska M, Denaro F, Rao S, Foulke J, Jones O, et al. An HIV-1 transgenic rat that develops HIV-related pathology and immunologic dysfunction. Proc Natl Acad Sci USA 2001;98:9271-6.
- 37. Roscoe RF, Mactutus CF, Booze RM. HIV-1 transgenic female rat: synaptodendritic alterations of medium spiny neurons in the nucleus accumbens. J Neuroimmune Pharmacol 2014;9:642-53.
- 38. Schier CJ, Marks WD, Paris JJ, Barbour AJ, McLane VD, Maragos WF, et al. Selective vulnerability of striatal D2 versus D1 dopamine receptor-expressing medium spiny neurons in HIV-1 Tat transgenic male mice. J Neurosci 2017;37:5758-69.
- 39. McLaurin KA, Cook AK, Li H, League AF, Mactutus CF, Booze RM. Synaptic connectivity in medium spiny neurons of the nucleus accumbens: a sex-dependent mechanism underlying apathy in the HIV-1 transgenic rat. Front Behav Neurosci 2018;12:285.
- 40. Kraemer HC, Yesavage JA, Taylor JL, Kupfer D. How can we learn about developmental processes from cross-sectional studies, or can we? Am J Psychiatr 2000;157:163 - 71.

- 41. Marcondes FK, Bianchi FJ, Tanno AP. Determination of the estrous cycle phases of rats: some helpful considerations. Braz | Biol 2002;62:609-14.
- 42. Li H, McLaurin KA, Mactutus CF, Booze RM. Ballistic labeling of pyramidal neurons in brain slices and in primary cell culture. J Vis Exp 2020;158. https://doi.org/10.3791/60989-v.
- 43. Paxinos G, Watson C. The rat brain in stereotaxic coordinates, 7th ed. Cambridge, MA: Elsevier Academic Press; 2014.
- 44. Fernández-Cabrera MR, Higuera-Matas A, Fernaud-Espinosa I, DeFelipe J, Ambrosio E, Miguéns M. Selective effects of Δ 9-tetrahydrocannabinol on medium spiny neurons in the striatum. PLoS One 2018;13:e0200950.
- 45. Shen H, Sesack SR, Toda S, Kalivas PW. Automated quantification of dendritic spine density and spine head diameter in medium spiny neurons of the nucleus accumbens. Brain Struct Funct 2008:213:149-57.
- 46. Akaza H. Prostate cancer chemoprevention by soy isoflavones: role of intestinal bacteria as the "second human genome". Cancer Sci 2012;103:969-75.
- 47. Berry KP, Nedivi E. Spine dynamics: are they all the same? Neuron 2017;96:43-55.
- 48. Mainen ZF, Sejnowski TJ. Influence of dendritic structure on firing pattern in model neocortical neurons. Nature 1996;382:363 – 6.
- 49. van der Velden L, van Hooft JA, Chameau P. Altered dendritic complexity affects firing properties of cortical layer 2/3 pyramidal neurons in mice lacking the 5-HT3A receptor. J Neurophysiol 2012;108:1521-8.
- 50. Smart IH. A pilot study of cell production by the ganglionic eminences of the developing mouse brain. J Anat 1976;121:71 – 84.
- 51. Fentress JC, Stanfield BB, Cowan WM. Observation on the development of the striatum in mice and rats. Anat Embryol 1981;163:275 - 98.
- 52. Bayer SA. Neurogenesis in the rat neostriatum. Int | Dev Neurosci 1984:2:163 - 75.
- 53. Deacon TW, Pakzaban P, Isacson O. The lateral ganglionic eminence is the origin of cells committed to striatal phenotypes: neural transplantation and developmental evidence. Brain Res
- 54. Nery S, Fishell G, Corbin JG. The caudal ganglionic eminence is a source of distinct cortical and subcortical cell populations. Nat Neurosci 2002:5:1279 - 87.
- 55. Halliday AL, Cepko CL. Generation and migration of cells in the developing striatum. Neuron 1992;9:15 – 26.
- 56. Tepper JM, Sharpe NA, Koós TZ, Trent F. Postnatal development of the rat neostriatum: electrophysiological, light- and electron-microscopic studies. Dev Neurosci 1998;20:125-45.
- 57. Lee H, Sawatari A. Medium spiny neurons of the neostriatal matrix exhibit specific, stereotyped changes in dendritic arborization during critical developmental period in mice. Eur J Neurosci 2011;34:1345-54.
- 58. Khodr CE, Chen L, Al-Harthi L, Hu XT. HIV-induced hyperactivity of striatal neurons is associated with dysfunction of voltage-gated calcium and potassium channels at middle age. Membranes 2022;12:737.
- 59. Kumar AM, Fernandez JB, Singer EJ, Commins D, Waldrop-Valverde D, Ownby RL, et al. Human immunodeficiency virus type 1 in the central nervous system leads to decreased dopamine in different regions of postmortem human brains. J Neurovirol 2009:15:257-74.

- 60. Javadi-Paydar M, Roscoe RF, Denton AR, Mactutus CF, Booze RM. HIV-1 and cocaine disrupt dopamine reuptake and medium spiny neurons in female rat striatum. PLoS One 2017;12:e0188404.
- 61. Denton AR, Samaranayake SA, Kirchner KN, Roscoe RF, Berger SN, Harrod SB, et al. Selective monoaminergic and histaminergic circuit dysregulation following long-term HIV-1 protein exposure. J Neurovirol 2019;25:540 - 50.
- 62. Denton AR, Mactutus CF, Lateef AU, Harrod SB, Booze RM. Chronic SSRI treatment reverses HIV-1 protein-mediated synaptodendritic damage. J Neurovirol 2021;27:403-21.
- 63. Harris KM, Jensen FE, Tsao B. Three-dimensional structure of dendritic spines and synapses in rat hippocampus (CA1) at postnatal day 14 and adult ages: implications for the maturation of synaptic physiology and long-term potentiation. | Neurosci 1992:12:2685-705.
- 64. Matsuzaki M, Ellis-Davies GC, Nemoto T, Miyashita Y, Iino M, Kasai H. Dendritic spine geometry is critical for AMPA receptor expression in hippocampal CA1 pyramidal neurons. Nat Neurosci 2001;4:1086-92.
- 65. Noguchi J, Matsuzaki M, Ellis-Davies GCR, Kasai H. Spine-neck geometry determines NMDA receptor-dependent Ca2+ signaling in dendrites. Neuron 2005;46:609-22.
- 66. Shin AH, Kim HJ, Thayer SA. Subtype selective NMDA receptor antagonists induce recovery of synapses lost following exposure to HIV-1 Tat. Br J Pharmacol 2012;166:1002-17.
- 67. Li H, McLaurin KA, Mactutus CF, Booze RM. Microglia proliferation underlies synaptic dysfunction in the prefrontal cortex: implications for the pathogenesis of HIV-1-associated neurocognitive and affective alterations. J Neurovirol 2023. https://doi.org/10.1007/s13365-023-01147-x [Epub ahead of print].
- 68. Haughey NJ, Nath A, Mattson MP, Slevin JT, Geiger JD. HIV-1 Tat through phosphorylation of NMDA receptors potentiates glutamate excitotoxicity. J Neurochem 2001;78:457 – 67.
- 69. Krogh KA, Wydeven N, Wickman K, Thayer SA. HIV-1 protein Tat produces biphasic changes in NMDA-evoked increases in intracellular Ca2+ concentration via activation of Src kinase and nitric oxide signaling pathways. J Neurochem 2014;130:
- 70. Niehrs C. The complex world of WNT receptor signalling. Nat Rev Mol Cell Biol 2012:13:767-79.
- 71. Stamos JL, Weis WI. The β-catenin destruction complex. Cold Spring Harbor Perspect Biol 2013;5:a007898.
- 72. Yu X, Malenka RC. Beta-catenin is critical for dendritic morphogenesis. Nat Neurosci 2003;6:1169-77.
- 73. Rosso SB, Sussman D, Wynshaw-Boris A, Salinas PC. Wnt signaling through dishevelled, rac and JNK regulates dendritic development. Nat Neurosci 2005;8:34-42.
- 74. Chailangkarn T, Trujillo CA, Freitas BC, Hrvoj-Mihic B, Herai RH, Yu DX, et al. A human neurodevelopmental model for Williams syndrome. Nature 2016;536:338-43.
- 75. Lanoue V, Langford M, White A, Sempert K, Fogg L, Cooper HM. The Wnt receptor Ryk is a negative regulator of mammalian dendrite morphogenesis. Sci Rep 2017;7:5965.
- 76. Ciani L, Boyle KA, Dickins E, Sahores M, Anane D, Lopes DM, et al. Wnt7a signaling promotes dendritic spine growth and synaptic strength through Ca²⁺/Calmodulin-dependent protein kinase II. Proc Natl Acad Sci USA 2011;108:10732 – 7.
- 77. Ramírez VT, Ramos-Fernández E, Henríguez JP, Lorenzo A, Inestrosa NC. Wnt-5a/Frizzled9 receptor signaling through the

- $G\alpha o$ - $G\beta \gamma$ complex regulates dendritic spine formation. J Biol Chem 2016;291:19092-107.
- 78. Inestrosa NC, Arenas E. Emerging roles of Wnts in the adult nervous system. Nat Rev Neurosci 2010;11:77 – 86.
- 79. Farías GG, Alfaro IE, Cerpa W, Grabowski CP, Godoy JA, Bonansco C, et al. Wnt-5a/JNK signaling promotes the clustering of PSD-95 in hippocampal neurons. | Biol Chem 2009;284:15857-66.
- 80. Cerpa W, Farías GG, Godoy JA, Fuenzalida M, Bonansco C, Inestrosa NC. Wnt-5a occludes abeta oligomer-induced depression of glutamatergic transmission in hippocampal neurons. Mol Neurodegener 2010;5:3.
- 81. Cao J, Wang S, Wang J, Cui W, Nesil T, Vigorito M, et al. RNA deep sequencing analysis reveals that nicotine restores impaired gene expression by viral proteins in the brains of HIV-1 transgenic rats. PLoS One 2013:8:e68517.
- 82. Coelho AVC, Gratton R, de Melo JPB, Andrade-Santos JL, Guimarães RL, Crovella S, et al. HIV-1 infection transcriptomics: meta-analysis of CD4+ T cells gene expression profiles. Viruses 2021;13:244.
- 83. Maggirwar SB, Tong N, Ramirez S, Gelbard HA, Dewhurst S. HIV-1 Tat-mediated activation of glycogen synthase kinase-3beta contributes to Tat-mediated neurotoxicity. J Neurochem 1999:73:578 - 86.
- 84. Masvekar RR, El-Hage N, Hauser KF, Knapp PE. GSK3 β -activation is a point of convergence for HIV-1 and opiate-mediated interactive neurotoxicity. Mol Cell Neurosci 2015;65:11-20.
- 85. Cardona-Gomez P, Perez M, Avila J, Garcia-Segura LM, Wandosell F. Estradiol inhibits GSK3 and regulates interaction of estrogen receptors, GSK3, and beta-catenin in the hippocampus. Mol Cell Neurosci 2004;25:363-73.

- 86. Varea O, Garrido JJ, Dopazo A, Mendez P, Garcia-Segura LM, Wandosell F. Estradiol activates beta-catenin dependent transcription in neurons. PLoS One 2009;4:e5153.
- 87. Quintanilla RA, Muñoz FJ, Metcalfe MJ, Hitschfeld M, Olivares G, Godoy JA, et al. Trolox and 17beta-estradiol protect against amyloid beta-peptide neurotoxicity by a mechanism that involves modulation of the Wnt signaling pathway. J Biol Chem 2005;280:11615-25.
- 88. Bhukhai K, Suksen K, Bhummaphan N, Janjorn K, Thongon N, Tantikanlayaporn D, et al. A phytoestrogen diarylheptanoid mediates estrogen receptor/Akt/glycogen synthase kinase 3β protein-dependent activation of the Wnt/β-catenin signaling pathway. J Biol Chem 2012;287:36168-78.
- 89. Wang Z, Chen H. Genistein increases gene expression by demethylation of WNT5a promoter in colon cancer cell line SW1116. Anticancer Res 2010;30:4537-45.
- 90. Gan WB, Grutzendler J, Wong WT, Wong RO, Lichtman JW. Multicolor "DiOlistic" labeling of the nervous system using lipophilic dye combinations. Neuron 2000;27:219-25.
- 91. Honig MG, Hume RI. Fluorescent carbocyanine dyes allow living neurons of identified origin to be studied in long-term cultures. J Cell Biol 1986;103:171-87.
- 92. O'Brien JA, Lummis SCR. Diolistics: incorporating fluorescent dyes into biological samples using a gene gun. Trends Biotechnol 2007;25:530-4.
- 93. Dickstein DL, Dickstein DR, Janssen WGM, Hof PR, Glaser JR, Rodriguez A, et al. Automatic dendritic spine quantification from confocal data with Neurolucida 360. Curr Protoc Neurosci 2016;77:1.27.1 - 21.